Biochemical and Biophysical Research Communications 439 (2013) 427–432

Contents lists available at ScienceDirect

Biochemical and Biophysical Research Communications

journal homepage: www.elsevier.com/locate/ybbrc

Recombinant production and solution structure of lipid transfer protein from lentil *Lens culinaris* ☆

Albina K. Gizatullina [a,b], Ekaterina I. Finkina [a], Konstantin S. Mineev [a], Daria N. Melnikova [a], Ivan V. Bogdanov [a], Irina N. Telezhinskaya [a,b], Sergey V. Balandin [a,b], Zakhar O. Shenkarev [a], Alexander S. Arseniev [a,b], Tatiana V. Ovchinnikova [a,b,*]

[a] *Shemyakin and Ovchinnikov Institute of Bioorganic Chemistry, Russian Academy of Sciences, Miklukho-Maklaya str., 16/10, 117997 Moscow, Russia*
[b] *Moscow Institute of Physics and Technology (State University), Department of Physicochemical Biology and Biotechnology, Institutskii per., 9, 141700, Dolgoprudny, Moscow Region, Russia*

ARTICLE INFO

Article history:
Received 21 August 2013
Available online 31 August 2013

Keywords:
Allergen
Antimicrobial peptide
Lipid transfer protein
Lentil
Lens culinaris
Recombinant expression
NMR
Spatial structure

ABSTRACT

Lipid transfer protein, designated as Lc-LTP2, was isolated from seeds of the lentil *Lens culinaris*. The protein has molecular mass 9282.7 Da, consists of 93 amino acid residues including 8 cysteines forming 4 disulfide bonds. Lc-LTP2 and its stable isotope labeled analogues were overexpressed in *Escherichia coli* and purified. Antimicrobial activity of the recombinant protein was examined, and its spatial structure was studied by NMR spectroscopy. The polypeptide chain of Lc-LTP2 forms four α-helices (Cys4-Leu18, Pro26-Ala37, Thr42-Ala56, Thr64-Lys73) and a long C-terminal tail without regular secondary structure. Side chains of the hydrophobic residues form a relatively large internal tunnel-like lipid-binding cavity (van der Waals volume comes up to ~600 Å^3). The side-chains of Arg45, Pro79, and Tyr80 are located near an assumed mouth of the cavity. Titration with dimyristoyl phosphatidylglycerol (DMPG) revealed formation of the Lc-LTP2/lipid non-covalent complex accompanied by rearrangements in the protein spatial structure and expansion of the internal cavity. The resultant Lc-LTP2/DMPG complex demonstrates limited lifetime and dissociates within tens of hours.

1. Introduction

In plants, lipids carry out many important functions including storage of energy, cell compartmentalization, protection, and signal transduction in different processes. Transfer of lipids such as free fatty acids, sterols, phospholipids and their derivatives in an aqueous environment of biological systems is facilitated by lipid binding proteins. These proteins belong to different families such as lipid transfer proteins (LTPs), sterol carrier proteins, puroindolines, and Bet v 1 homologues. Plant LTPs constitute a family of small water-soluble and mostly basic proteins that are able to bind and transfer a variety of hydrophobic ligands *in vitro* [1]. These proteins are classified into two subfamilies according to their molecular masses: LTP1s (~9 kDa) and LTP2s (~7 kDa) [2]. Plant LTPs have an extracellular location, generally at the periphery of plant organs, and are synthesized as precursors composed of a signal peptide of 20–25 amino acids and a mature protein [3]. Different LTP isoforms are expressed in various organs and tissues at certain stages of ontogeny [1]. The biological role of LTPs still remains a matter of debate. It has been proposed that these proteins are involved in plant response to abiotic and biotic stresses [4], cutin and suberin formation [5], somatic embryogenesis [6] and could play the role of systemic signaling molecules [7].

Spatial structures of plant LTP1s, determined by X-ray crystallography or NMR spectroscopy, are composed of four α-helices linked by flexible loops and a long C-terminal tail [8–12]. The overall LTP1s structure is stabilized by four disulfide bridges and characterized by the presence of large tunnel-like hydrophobic cavity with space sufficient for binding of one or two lipid molecules [13]. Hydrophobic interactions play a major role in lipid binding. Plant LTP1s bind a broad range of hydrophobic molecules including fatty acids, ranging from C10 to C18 [14], phospholipids [15,16], lyso-derivatives [10], prostaglandin B2 [11], and acyl-coenzyme A [17]. Although plant LTP1s exhibit similar global folds, their lipid binding capacity depends on shape and volume of the internal cavity, amino acids localized in the internal cavity, and tenuous variations in the organization of secondary structure elements [5]. The capacity of LTP1s to withdraw lipids from micelles or bilayers also varies from one protein to another [18]. LTPs ligand-binding modes, established by NMR or X-ray analysis,

☆ The atomic coordinates and structure factors have been deposited in the Worldwide Protein Data Bank (PDB ID 2LJO).

* Corresponding author at: Shemyakin and Ovchinnikov Institute of Bioorganic Chemistry, Russian Academy of Sciences, Miklukho-Maklaya str., 16/10, 117997, Moscow, Russia. Fax: +7 495 336 43 33.
E-mail addresses: ovch@ibch.ru, ovch@bk.ru (T.V. Ovchinnikova).

0006-291X/$ - see front matter © 2013 Elsevier Inc. All rights reserved.
http://dx.doi.org/10.1016/j.bbrc.2013.08.078

differ from each other, and various orientations of hydrophobic ligands are reported for plant LTP1s [14–17]. A systematic analysis of three-dimensional structures of plant LTPs can contribute to a better understanding of variability of their properties and multiple functions of these proteins.

Earlier we found a subfamily of eight proteins, designated as Lc-LTP1-8, in *Lens culinaris* [19]. The sequences of these proteins allow to classify them as the lipid transfer proteins belonging to the LTP1s family. Four isoforms (Lc-LTP2, 4, 7, 8) exhibiting antibacterial activity were purified from the lentil germinated seeds, and their complete amino acid sequences were determined. Besides, Lc-LTP2 was characterized as a new lentil allergen Len c 3 [20]. Here we report the bacterial expression system for production of the recombinant Lc-LTP2 and its ^{15}N- and ^{13}C, ^{15}N-labeled analogues. Antimicrobial activity, spatial structure, and interaction of the recombinant Lc-LTP2 with DMPG lipid were studied in the present work.

2. Materials and methods

2.1. Heterologous expression, purification and characterization of recombinant Lc-LTP2 and its ^{15}N- and ^{13}C, ^{15}N-labeled analogues

The recombinant Lc-LTP2 was expressed and purified as described [20] with some modifications (see Supporting Information: Experimental Procedures). ^{15}N- and ^{13}C, ^{15}N-labeled Lc-LTP2 were expressed in M9 minimal medium containing 1 g/L $^{15}NH_4Cl$ (CIL) or $^{15}NH_4Cl$ and [U-$^{13}C_6$]glucose (CIL), respectively. The recombinant Lc-LTP2 and its ^{15}N- and ^{13}C, ^{15}N-labeled analogues were analyzed by SDS–PAGE, MALDI mass spectrometry (Reflex III Mass Spectrometer, Bruker Daltonics), and automated microsequensing (Procise cLC 491 Protein Sequencing System, PE Applied Biosystems).

2.2. Antimicrobial assay

Antimicrobial activity of the recombinant Lc-LTP2 was measured by microspectrophotometry using 96-well microplates and serial dilution as described [19,20]. The phytopathogenic bacteria and fungi were obtained from the All-Russian Collection of Microorganisms (Pushchino, Russia). The IC_{50} was defined as the lowest protein concentration that causes at least 50% growth inhibition after 24 or 48 h of incubation in case of bacteria or fungi, correspondingly. Spore germination and morphology of hyphae were observed with an Olympus CKX41 microscope after 12 and 24 h of spore suspension incubation (in half-strength potato glucose broth) at 25 °C in the presence of water (as a control) or the protein solutions.

2.3. NMR experiments and spatial structure calculation

NMR investigation was done using 1.0–1.5 mM samples of the unlabeled recombinant Lc-LTP2 and its ^{15}N- or ^{15}N, ^{13}C-labeled analogues in deuterated 20 mM sodium acetate buffer solution (pH 5.6, d4-acetic acid, CIL, USA) containing 5% or 100% D_2O. NMR spectra were acquired on Bruker Avance III 600 and 800 spectrometers equipped with cryoprobes at 30 °C. ^{1}H, ^{13}C, and ^{15}N resonance assignment of Lc-LTP2 was obtained by a standard procedure based on combination of triple-resonance 3D HNCO, HNCACB, and 2D or 3D isotopically edited TOCSY and NOESY spectra. 3D ^{13}C-NOESY-HSQC and H(C)CH-HSQC-TOCSY-HSQC were acquired using non-uniform sampling (NUS) scheme and processed in qMDD software [21]. The $^3J_H{}^N{}_H{}^\alpha$, $^3J_{NH}{}^\beta$ and $^3J_{NH}{}^\alpha$ coupling constants were measured using 3D HNHA and HNHB experiments [22]. The $^3J_H{}^\alpha{}_H{}^\beta$ coupling constants were measured using unlabeled Lc-LTP2 sample in 100% D_2O by the ACME program in the COSY spectrum [23]. $^3J_C{}^\gamma{}_C$, $^3J_C{}^\gamma{}_N$ constants for Val, Ile, and Thr residues were quantitatively calculated from the cross-peak intensities in the spin-echo difference ^{13}C-HSQC experiments [22].

Spatial structure calculation was performed in the CYANA 3.0 program [24]. Upper interproton distance constraints were derived from the intensities of cross-peaks in 3D ^{15}N-NOESY-HSQC and ^{13}C-NOESY-HSQC (τ_m = 80 ms) spectra via a "$1/r^6$" calibration. ^{1}H, ^{13}C, and ^{15}N backbone chemical shifts were used as an input for the TALOS + software to predict the secondary structure and backbone intramolecular mobility [25]. Torsion angle restraints and stereospecific assignments were obtained from *J* coupling constants, NOE intensities and TALOS + predictions. Hydrogen bonds were introduced basing on deuterium exchange rates of H^N protons. The disulfide bond connectivity pattern was established on the basis of the observed NOE contacts and verified during preliminary stages of the spatial structure calculation. The location and volume of the cavities in the proteins were calculated using CASTp with a 1.4 Å probe radius [26].

Titration of 0.5 mM ^{15}N-labeled Lc-LTP2 sample with multilamellar DMPG vesicles was performed at 30 °C. At each lipid concentration (0.3 mM, 0.6 mM, 0.9 mM, 2.1 mM) 1D ^{1}H and 2D ^{15}N-HSQC spectra were acquired. Additionally 3D ^{15}N-NOESY-HSQC (τ_m = 80 ms) and HNHA spectra were recorded at 2.1 mM concentration of DMPG.

3. Results

3.1. Heterologous expression, purification and characterization of recombinant Lc-LTP2 and its stable isotope labeled analogues

E. coli BL-21(DE3) cells were transformed by pET-His8-TrxL-Lc-LTP2, containing Lc-LTP2 sequence fused with thioredoxin A (M37L) as a carrier protein. Decreasing the induction temperature down to 25–30 °C resulted in increasing level of the Lc-LTP2-containing fusion protein in a soluble form. In LB medium the final yield of purified Lc-LTP2 was estimated to be 5 mg/L of cell culture.

In order to obtain uniformly ^{15}N- and ^{13}C, ^{15}N-labeled recombinant Lc-LTP2, the BL-21 (DE3) cells transformed with the same plasmid were grown in minimal medium, containing $^{15}NH_4Cl$ and [U-$^{13}C_6$]glucose as the only nitrogen and carbon sources. In M9 minimal medium yields of the ^{15}N- and ^{13}C, ^{15}N-labeled recombinant proteins were somewhat lower (4.0 and 3.5 mg/L, respectively).

Purification of the recombinant Lc-LTP2 was carried out by IMAC, subsequent dialysis and CNBr cleavage of the fusion protein, elimination of the carrier protein by subtractive IMAC, and final RP-HPLC.

The recombinant Lc-LTP2 was proved to be identical to the natural protein (molecular masses of 9282.4 Da and 9282.7 Da, respectively). The ^{15}N- and ^{13}C, ^{15}N-labeled analogues showed 113 and 508 Da increase in molecular mass (9395.1 and 9790.4 Da, respectively) indicating that all the ^{14}N and ^{12}C atoms were substituted with stable isotopes ^{15}N and ^{13}C.

3.2. Biological activity of the recombinant Lc-LTP2

Antimicrobial activity of the recombinant Lc-LTP2 was examined by the broth microdilution assay. Lc-LTP2 was active against most of phytopathogenic bacteria and fungi tested but at rather high inhibitory concentrations (Table 1). Lc-LTP2 inhibited spore germination and slowed down hyphae elongation of the sensitive microorganisms, but did not induce any morphological distortions. *Aspergillus niger*, strain VKM F-2259, and *Botrytis cinerea*, strain VKM F-3700, which cause plant diseases called black

Table 1
Antimicrobial activity of Lc-LTP2.

Test microorganisms	IC_{50}, μM
Bacteria	
Agrobacterium tumefaciens, strain A281	20–40
Clavibacter michiganensis, strain VKM Ac-1144	>40
Pseudomonas syringae, strain VKM B-1546	>40
Fungi	
Alternaria alternata, strain VKM F-3047	>40
Aspergillus niger, strain VKM F-2259	10–20
Aspergillus versicolor, strain VKM F-1114	na
Botrytis cinerea, strain VKM F-3700	10–20
Fusarium culmorum, strain VKM F-844	na
Fusarium solani, strain VKM F-142	>40
Neurospora crassa, strain VKM F-184	20–40

na = not active.

and gray mold, were the most sensitive test microorganisms to Lc-LTP2.

3.3. Spatial structure of Lc-LTP2

Spatial structure of Lc-LTP2 was determined by heteronuclear NMR spectroscopy in aqueous solution (Fig. 1A, and Fig. 2). The characteristic $d_{\alpha N}(i, i+3)$ and $d_{\beta N}(i, i+3)$ NOE contacts, amide proton exchange rates and values of $^{3}J_{H^N H^\alpha}$ coupling constants reveal that the protein molecule involves four α-helices: Cys4-Leu18 (H1), Pro26-Ala37 (H2), Thr42-Ala56 (H3), Thr64-Lys73 (H4) and a long C-terminal tail (Gly75-Phe93) without regular secondary structure. The helix H1 demonstrates a pronounced kink at Pro13. Probability of helix conformation (Helix_p) and random coil index order parameters (RCI-S^2) calculated in TALOS+ [25] were in agreement with the established secondary structure. The lower RCI-S^2 values were observed in the loop regions which are characterized by increased mobility (Fig. 2). The *cis* orientation of the Gly23–Pro24 peptide bond was established on the basis of sequential NOE cross-peaks.

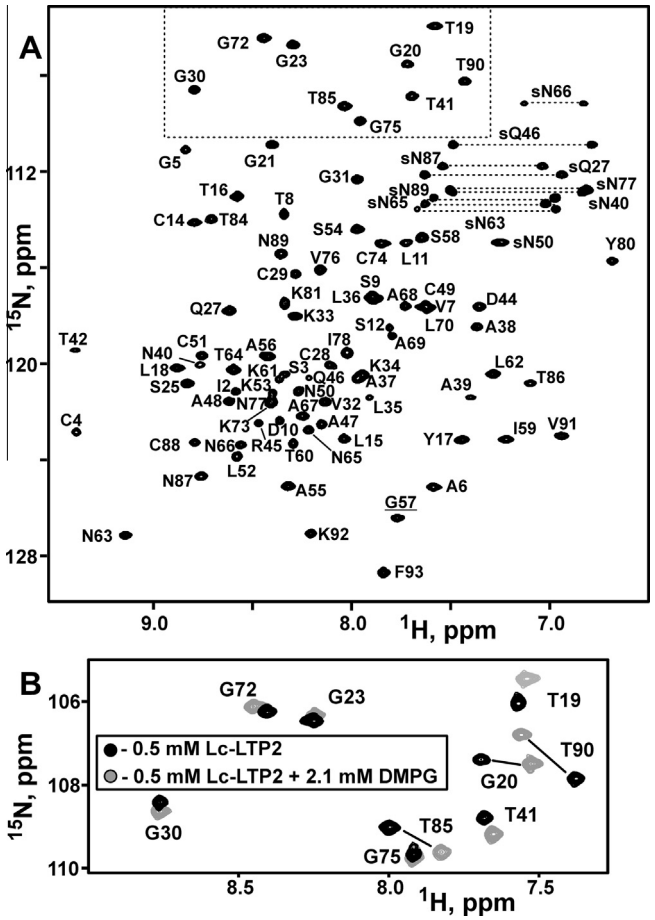

Fig. 1. (A) 2D ^{1}H, ^{15}N-HSQC spectrum of Lc-LTP2 (0.5 mM, pH 5.6, 30 °C). The "folded" resonances are underlined. (B) The fragments of Lc-LTP2 spectra the absence (black) or in the presence (gray) of DMPG. The corresponding spectral region is marked by dashed rectangle on the panel A.

The set of 20 Lc-LTP2 spatial structures (Fig. 3A) was calculated in CYANA from 200 random starts using the following experimental data: upper and lower NOE based distance restraints, J coupling based torsion angle restraints and hydrogen bond restraints (Table S1). The protein structure is stabilized by four disulfide bonds (Cys4-Cys51, Cys14-Cys28, Cys29-Cys74, Cys49-Cys88) and 32 hydrogen bonds. The moderate divergence of the calculated structural ensembles in the C-terminal tail (Gly75-Phe93) (Fig. 3A) is probably connected with the enhanced intramolecular mobility of this segment. Implementation of ^{13}C-labeling allowed to detect a number of medium- and long-range NOE contacts between aliphatic protons of Lc-LTP2, which significantly increased the quality and reliability of the determined spatial structure (Table S1).

In the determined Lc-LTP2 spatial structure (Fig. 3B) the first three helices (H1–H3) form a parallel bundle having an overall boat-like shape with the interior lined with apolar side chains. This hydrophobic cavity is shielded from the aqueous environment by the H4 helix and the C-terminal tail. Similarly to other LTP1s, this cavity may play a role in lipids binding to the protein. The outer surface of Lc-LTP2 is lined by polar and charged residues, and does not contain pronounced hydrophobic patches that could be used for membrane anchoring (Fig. 3C).

3.4. Interaction of Lc-LTP2 with DMPG

Interaction of the protein with multilamellar dimyristoyl phosphatidylglycerol (DMPG) vesicles was studied by NMR spectroscopy. Two sets of the cross-peaks (corresponding to the lipid-free and lipid-bound protein) were observed in ^{15}N-HSQC spectra of Lc-LTP2 upon addition of the liposomes. The exchange cross-peaks observed in the NOESY spectrum of the Lc-LTP2/DMPG complex revealed that the characteristic time of the lipid binding/dissociation process is ~0.1–0.5 s (more precise calculation was impossible due to low stability of the complex, see below). The dissociation constant of the Lc-LTP2/DMPG complex could not be accurately determined from the available NMR data, but at the DMPG/Lc-LTP2 molar ratio exceeding unity, the signals of the lipid-free protein were not observed, indicating almost complete lipid binding (Fig. 1B).

The Lc-LTP2/DMPG complex demonstrated limited stability. After 2 days of NMR measurements ~50% of the protein was converted back to the lipid-free form, and substantial fraction of the lipid in the sample was precipitated. The obtained backbone ^{1}H and ^{15}N resonance assignment revealed that the lipid binding significantly perturbs the chemical shifts in all the parts of the Lc-LTP2 molecule (Fig. S1A). The largest chemical shifts changes ($\Delta\delta^{1}H^{15}N$) were observed in three spatially adjoined protein fragments (Fig. 3D): (1) the N-terminus of the helix H1 (Cys4-Ser12); (2) the C-terminus of H2, the H2-H3 loop, the entire H3, the H3-H4 loop, and the N-terminus of H4 (Lys33-Ala68); (3) the fragment of the C-terminal tail (Asn77-Lys92).

Comparison of the $^{3}J_{H^\alpha H^N}$ coupling constants (Fig. S1B) and relative intensities of amide group signals in ^{15}N-HSQC spectra (Fig. S1C) revealed the changes in the conformation and dynamics of the Lc-LTP2 backbone induced by the lipid binding. The largest difference in $^{3}J_{H^\alpha H^N}$ couplings (amplitude > 1.5 Hz) and ^{1}H–^{15}N

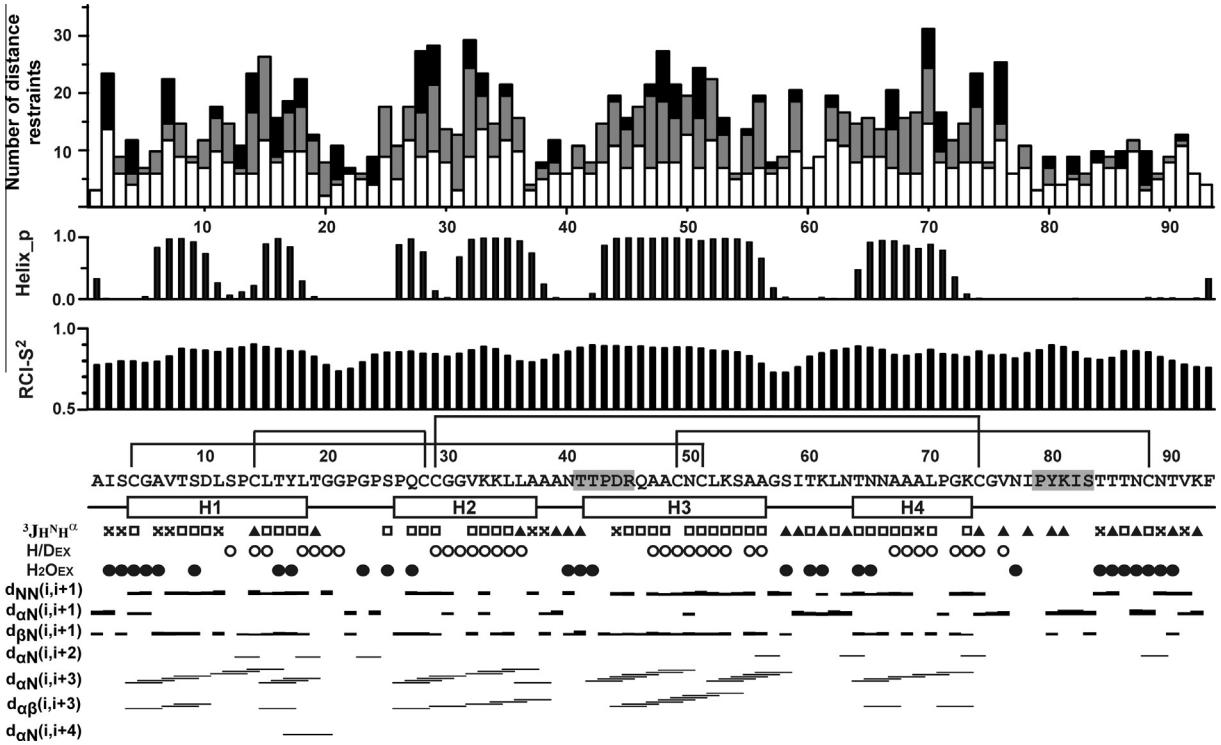

Fig. 2. Overview of NMR data collected for Lc-LTP2. (From top to bottom) Short range (intraresidual and sequential), medium-range ($1 < |i - j| \leqslant 4$) and long-range ($|i - j| > 4$) NOE distance restraints are designated by white, gray, and black rectangles, respectively. Probability of helix conformation (Helix_p) and random coil index order parameters (RCI-S^2) were calculated TALOS+. Large (>8 Hz), small (<6 Hz) and medium (others) $^3J_{H^N H^\alpha}$ couplings are indicated by the filled triangles, open squares, and crosses, respectively. The open circles (H/D_{EX}) denote H^N protons with H-D half-exchange time >30 min. Amide protons which demonstrate fast exchange with water protons are shown by filled circles (H_2O_{EX}). The corresponding cross-peaks on the water frequency were observed in the 3D ^{15}N-TOCSY-HSQC spectrum (τ_m = 80 ms). NOE connectivities correspond to cross-peaks observed in the 80 ms 3D NOESY spectra.

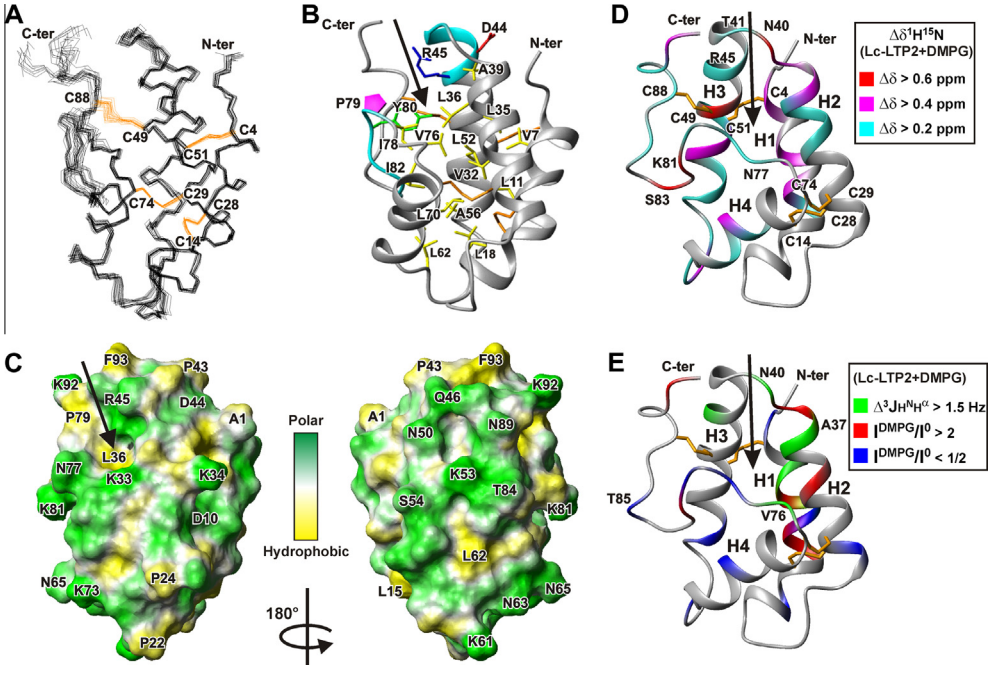

Fig. 3. (A) The calculated set of the 20 Lc-LTP2 structures. Cysteines are colored in orange. (B) Spatial structure of Lc-LTP2. Backbone of two pentapeptide fragments (Thr41-Arg45, Pro79-Ser83) and conservative Asp44, Arg45, Pro79, and Tyr80 residues are colored in cyan, red, blue, magenta, and green, respectively. The inwardly pointing hydrophobic residues which form the lipid-binding cavity are colored in yellow. (C) Two-sided view of molecular hydrophobicity potential on the Lc-LTP2 surface. (D,E) The Lc-LTP2 ribbon is colored according to the changes in ^{1}H-^{15}N chemical shifts ($\Delta\delta^1H^{15}N$), $^3J_{H^N H^\alpha}$ coupling constants ($\Delta^3J_{H^\alpha H^N}$), and intensities of HSQC cross-peaks (I^{DMPG}/I^0) upon DMPG binding. Please note that for Ala37, Asn40, and Val76 both $^3J_{H^N H^\alpha}$ and intensity of HSQC cross-peaks were changed significantly. The orientation of the Lc-LTP2 molecule on the panels D and E differs from one on the other panels. The expected entrance into internal hydrophobic cavity is shown by arrow. (For interpretation of the reference to color in this figure legend, the reader is referred to the web version of this article.)

cross-peak intensities (>2 times) were localized approximately at the same protein segments where large variation in $^{1}H–^{15}N$ chemical shifts was observed (Fig. 3E). Qualitative analysis of the recorded 3D ^{15}N-NOESY-HSQC spectrum indicated that the lipid binding decreased the number and magnitude of the interresidual contacts between methyl and NH groups of the protein (data not shown). This provides evidence in favor of expansion of the protein internal hydrophobic cavity upon the Lc-LTP2/DMPG complex formation.

4. Discussion

The presently obtained data revealed significant structural similarity of the Lc-LTP2 from *Lens culinaris* to the LTP1s from other plants. Analogously to other proteins, Lc-LTP2 encompasses four α-helices (H1-H4) which surround the internal hydrophobic cavity containing the lipid-binding site, and followed by a long C-terminal tail (Fig 3). Lc-LTP2 can be fairly good superimposed (RMSD from 0.6 to 1.7 Å, over C^{α} atoms of the eight conserved cysteines) with the unliganded and liganded LTP1s from various plants, including barley, mung bean, tobacco, rice, maize, and wheat (Table S2). At the same time, the comparison revealed the differences in relative orientation of the interhelical loops and the C-terminal tail (Fig. S2).

Plant LTPs are well known for their ability to bind lipids in a non-covalent way and transfer them between membranes *in vitro*. However, the formation of the protein/lipid non-covalent complexes and the transfer of lipids *in vivo* are still obscure. The only plant LTP/lipid complex was isolated from barley. Post-translationally modified isoform of barley LTP1, named LTP1b, has been found to be covalently bound to a lipid adduct (*cis*-7-heptadecenoic acid [27] or α-ketol 9-hydroxy-10-oxo-12 (Z)-octadecenoic acid [28]) via the side chain of Asp7. In this study, formation of the Lc-LTP2/DMPG non-covalent complex, accompanied by rearrangements in the protein spatial structure and expansion of the internal cavity, was revealed by NMR spectroscopy. It is generally assumed that the lipid-binding/transfer activity of LTP1s is related to the organization of the hydrophobic cavity [1]. In contrast to other unliganded LTP1s having relatively small internal cavities (van der Waals volume ranges from 80 to 300 $Å^3$; Table S2), the lipid-free Lc-LTP2 holds much larger hollow space (~600 $Å^3$), which comprises about 7% of the total protein volume (~8600 $Å^3$, Fig. S3). However, this space is insufficient to accommodate double-chain lipid, which requires ~1100 $Å^3$ (in the case of DMPG). Indeed, the obtained experimental data point to the possible expansion of the Lc-LTP2 cavity upon the DMPG binding. This indicates that dimensions of the cavity could adjust to the volume of the bound ligand. Analysis of the liganded LTP1s revealed internal cavities with volumes in range from 650 to 1350 $Å^3$ which is in agreement with the above supposition (Table S2).

One of the most surprising results of the present investigation is limited lifetime of the Lc-LTP2/DMPG complex (half-life time <40 h). This makes difficulties in the detailed NMR investigation of the complex structure. Previously the interaction of LTP1 extracted from wheat seeds with DMPG vesicles was studied by NMR and fluorescence spectroscopy [16]. Nevertheless, the resulting complex was stable enough for structural investigation by 2D NMR [16]. The observed difference in stability of the LTP/lipid complexes could be connected with the differences in the organization of the hydrophobic cavities. Probably, the tighter cavity of the wheat LTP1 (~190 $Å^3$ in unliganded state) provides more energetically favorable contacts with the bound lipid, thus reducing dissociation rate. Relative instability of LTP/lipid non-covalent complexes may be the necessary condition for effective lipids transfer by LTPs and, simultaneously, the reason why such complexes were not detected *in vivo*.

The NMR spectral parameters (chemical shifts, intensity of signals, and *J* couplings) permit to track qualitatively the changes in the conformation and dynamics of Lc-LTP2 upon lipid binding (Fig. 3D and E). One side of the protein molecule, encompassing the H1-H2 loop (including the C-terminus of H1, and the N-terminus of H2) and the helix H4, demonstrates minor perturbations. In contrast to that, the opposite side of Lc-LTP2 is strongly affected by the bound lipid (Fig. 3D and E). This site of the protein surface accommodates two conserved pentapeptides (T/S-X-X-D-R/K and P-Y-X-I-S; T^{41}TPDR^{45} and P^{79}YKIS^{83} in case of Lc-LTP2; Fig. 2, gray, Fig. 3B, cyan), which, as proposed, contribute significantly to the lipid binding by interactions with the polar head groups [2,14]. In the lipid-free Lc-LTP2 the side chains of the conserved Arg45, Pro79, and Tyr80 residues restrict an expected entrance into the hydrophobic cavity (Fig. 3B, D and E, arrow).

The recombinant Lc-LTP2 has also been shown to possess non-specific antimicrobial activity against fytopathogenic fungi and bacteria decreasing their growth and generation. Neverthelss, even the highest concentration of Lc-Ltp2 used did not cause lysis of the fytopathogens tested. Correlation of these data with the lack of a marked amphiphilicity of the Lc-LTP2 molecule allows to propose its mechanism of action. Presumably, Lc-LTP2 as a cationic protein binds to the negatively charged components of biological membranes of fytopathogens. The local surface accumulation of Lc-LTP2 modifies the spontaneous curvature and destabilizes the membrane structure. This model essentially embodies a carpet-like mode of action of antimicrobial peptides on the lipid bilayer, and a lipid-binding activity of LTPs may be directly involved in such a membrane destabilization.

In summary, we characterized a recently discovered lipid transfer protein Lc-LTP2 from Lens culinaris by biological and structural methods. Earlier we characterized Lc-LTP2 as a new lentil allergen Len c 3 [20]. Knowledge of spatial structure of this protein is required for further studies of its antigenicity, IgE binding activity and localization of the conformational epitopes.

Acknowledgments

The reported study was partially supported by the Russian Foundation for Basic Research (projects Nos. 12-04-01224 and 13-08-00956), the Russian Federal Target Program "Scientific and Science-Educational Personnel of Innovative Russia" (project No. 8043), and the Russian Academy of Sciences (the program "Molecular and Cellular Biology").

Appendix A. Supplementary data

Supplementary data associated with this article can be found, in the online version, at http://dx.doi.org/10.1016/j.bbrc.2013.08.078.

References

[1] A.O. Carvalho, V.M. Gomes, Role of plant lipid transfer proteins in plant cell physiology – a concise review, Peptides 28 (2007) 1144–1153.
[2] J.P. Douliez, T. Michon, K. Elmorjani, D. Marion, Mini review: structure, biological and technological functions of lipid transfer proteins and indolines, the major lipid binding proteins from cereal kernels, J. Cer. Sci. 32 (2000) 1–20.
[3] V. Arondel, C. Vergnolle, C. Cantrel, J.C. Kader, Lipid transfer proteins are encoded by a small multigene family in *Arabidopsis thaliana*, Plant Sci. 157 (2000) 1–12.
[4] A.G. Gonorazky, M.C. Regente, L. de la Canal, Stress induction and antimicrobial properties of a lipid transfer protein in germinating sunflower seeds, J. Plant Physiol. 162 (2005) 618–624.
[5] M. Renan, J. Francois, M. Didier, M. Axelos, J.P. Douliez, Study of the interaction between end-capped telechelic polymers and the wheat lipid transfer protein LTP1, in solution and in the air/water interface, Coloids Surf. B: Biointerfaces 32 (2003) 213–221.
[6] P. Sterk, H. Booij, G.A. Schellekens, A. Van Kammen, S.C. De Vries, Cell-specific expression of the carrot EP2 lipid transfer protein gene, Plant Cell 3 (1991) 907–921.

[7] J.P. Blein, P. Coutos-Thevenot, D. Marion, M. Ponchet, From elicitins to lipid-transfer proteins: a new insight in cell signalling involved in plant defense mechanisms, Trends Plant Sci. 7 (2002) 293–296.

[8] K.F. Lin, Y.N. Liu, S.T.D. Hsu, D. Samuel, C.S. Cheng, A.M.J.J. Bonvin, P.C. Lyu, Characterization and structural analyses of nonspecific lipid transfer protein 1 from mung bean, Biochemistry 44 (2005) 5703–5712.

[9] P.D. Silva, C. Landon, B. Industri, A. Marais, D. Marion, M. Ponchet, F. Vovelle, Solution structure of a tobacco lipid transfer protein exhibiting new biophysical and biological features, Proteins 59 (2005) 356–367.

[10] J. Gomar, M.C. Petit, P. Sodano, S.Y. Denise, D. Marion, J.C. Kader, F. Vovelle, M. Ptak, Solution structure and lipid binding of a nonspecific lipid transfer protein extracted from maize seeds, Protein Sci. 5 (1996) 565–577.

[11] S. Tassin-Moindrot, A. Caille, J.P. Douliez, D. Marion, F. Vovelle, The wide binding properties of a wheat nonspecific lipid transfer protein. Solution structure of a complex with prostaglandin B2, Eur. J. Biochem. 267 (2000) 1117–1124.

[12] J.Y. Lee, K. Min, H. Cha, D.H. Shin, K.Y. Hwang, S.W. Suh, Rice non-specific lipid transfer protein: the 1.6 A crystal structure in the unliganded state reveals a small hydrophobic cavity, J. Mol. Biol. 276 (1998) 437–448.

[13] J.C. Kader, Lipid-transfer proteins in plants, Annu. Rev. Plant Physiol. Plant Mol. Biol. 47 (1996) 627–654.

[14] G.W. Han, J.Y. Lee, H.K. Song, C. Chang, K. Min, J. Moon, D.H. Shin, M.L. Kopka, M.R. Sawaya, H.S. Yuan, Structure basis of non-specific lipid binding in maize lipid-transfer protein complexes revealed by high-resolution X-ray crystallography, J. Mol. Biol. 308 (2001) 263–278.

[15] D. Charvolin, J.P. Douliez, D. Marion, C. Cohen-Addad, E. Pebay-Peyroula, The crystal structure of a wheat nonspecific lipid transfer protein (ns-LTP1) complexed with two molecules of phospholipid at 2.1 Å resolution, Eur. J. Biochem. 264 (1999) 562–568.

[16] P. Sodano, A. Caille, D. Sy, G. de Person, D. Marion, M. Ptak, 1H NMR and fluorescence studies of the complexation of DMPG by wheat non-specific lipid transfer protein. Global fold of the complex, FEBS Lett. 416 (1997) 130–134.

[17] M.H. Lerche, B.B. Kragelund, L.M. Bech, F.M. Poulsen, Barley lipid-transfer protein complexed with palmitoyl CoA: the structure reveals a hydrophobic binding site that can expand to fit both large and small lipid-like ligands, Structure 5 (1997) 291–306.

[18] M. Subirade, C. Salesse, D. Marion, M. Pezolet, Interaction of a nonspecific wheat lipid transfer protein with phospholipid monolayers imaged by fluorescence microscopy and studied by infrared spectroscopy, Biophys. J. 69 (1995) 974–988.

[19] E.I. Finkina, S.V. Balandin, M.V. Serebryakova, N.A. Potapenko, A.A. Tagaev, T.V. Ovchinnikova, Purification and primary structure of novel lipid transfer proteins from germinated lentil (*Lens culinaris*) seeds, Biochemistry (Mosc.) 72 (2007) 430–438.

[20] J. Akkerdaas, E.I. Finkina, S.V. Balandin, S. Santos Magadán, A. Knulst, M. Fernandez-Rivas, R. Asero, R. van Ree, T.V. Ovchinnikova, Lentil (*Lens culinaris*) lipid transfer protein Len c 3, a novel legume allergen, Int. Arch. Allergy Immunol. 157 (2012) 51–57.

[21] V.Y. Orekhov, V.A. Jaravine, Analysis of non-uniformly sampled spectra with multi-dimensional decomposition, Prog. Nucl. Magn. Reson. Spectrosc. 59 (2011) 271–292.

[22] A. Bax, G.W. Vuister, S. Grzesiek, F. Delaglio, A.C. Wang, R. Tschudin, G. Zhu, Measurement of homo- and heteronuclear J couplings from quantitative J correlation, Methods Enzymol. 239 (1994) 79–105.

[23] F. Delaglio, Zh. Wu, A. Bax, Measurement of homonuclear proton couplings from regular 2D COSY spectra, J. Magn. Reson. 149 (2001) 276–281.

[24] P. Guntert, Automated NMR structure calculation with CYANA, Method Mol. Biol. 278 (2004) 353–378.

[25] Y. Shen, F. Delaglio, G. Cornilescu, A. Bax, TALOS+: A hybrid method for predicting protein backbone torsion angles from NMR chemical shifts, J. Biomol. NMR 44 (2009) 213–223.

[26] J. Dundas, Z. Ouyang, J. Tseng, A. Binkowski, Y. Turpaz, J. Liang, CASTp: computed atlas of surface topography of proteins with structural and topographical mapping of functionally annotated residues, Nucleic Acid Res. 34 (2006) W116–W118.

[27] K. Lindorff-Larsen, M.H. Lerche, F.M. Poulsen, P. Roepstorff, J.R. Winther, Barley lipid transfer protein, LTP1, contains a new type of lipid-like post-translational modification, J. Biol. Chem. 276 (2001) 33547–33553.

[28] B. Bakan, M. Hamberg, L. Perrocheau, D. Maume, H. Rogniaux, O. Tranquet, C. Rondeau, J.P. Blein, M. Ponchet, D. Marion, Specific adduction of plant lipid transfer protein by an allene oxide generated by 9-lipoxygenase and allene oxide synthase, J. Biol. Chem. 281 (2006) 38981–38988.